Volume 36
Number 12
December 2021
Pages 2563–2764

JAAS

Journal of Analytical Atomic Spectrometry

rsc.li/jaas

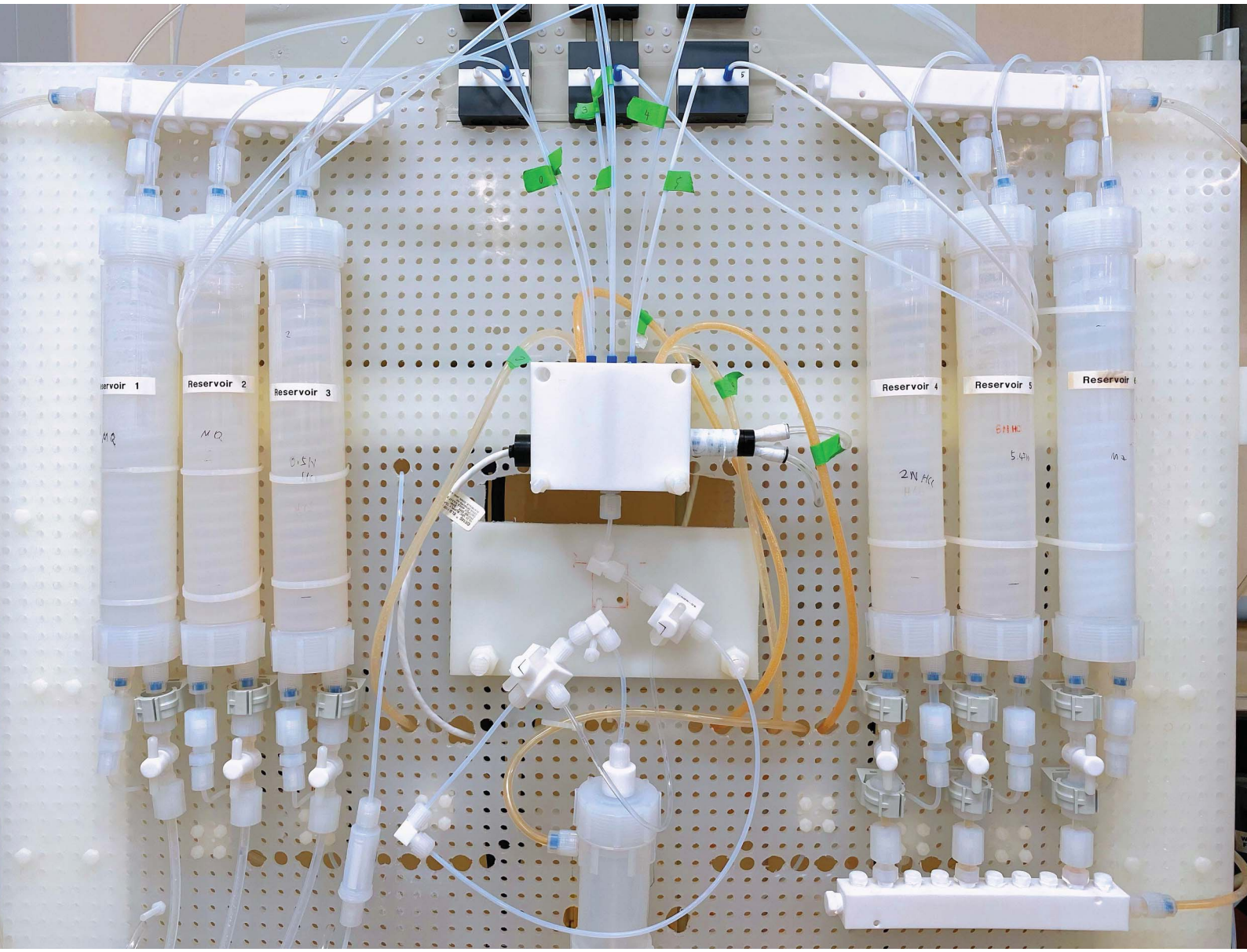

ISSN 0267-9477

ROYAL SOCIETY OF CHEMISTRY

PAPER

Nicole X. Nie *et al.*

Chromatography purification of Rb for accurate isotopic analysis by MC-ICPMS: a comparison between AMP-PAN, cation-exchange, and Sr resins

JAAS

ROYAL SOCIETY OF CHEMISTRY

PAPER

View Article Online
View Journal | View Issue

Cite this: *J. Anal. At. Spectrom.*, 2021, **36**, 2588

Chromatography purification of Rb for accurate isotopic analysis by MC-ICPMS: a comparison between AMP-PAN, cation-exchange, and Sr resins

Nicole X. Nie, *[ab] Nicolas Dauphas,[a] Timo Hopp, [a] Justin Y. Hu, [a] Zhe J. Zhang,[a] Reika Yokochi,[a] Thomas J. Ireland[ac] and Francois L. H. Tissot [ad]

The isotopic compositions of alkali metal elements are powerful tracers of various geological processes. Coupled K and Rb isotopic studies can potentially yield new clues on the mechanisms responsible for the depletions in moderately volatile elements in planetary objects, global surface geochemical cycles, and mechanistic aspects of water–rock interactions. Rubidium isotopic studies have however been hampered by difficulties in purifying Rb from rocks, notably due to its similar chemical behavior to K. Here we characterize the properties of three different types of resins (AMP-PAN resin; AG50W-X8 and AG50W-X12 cation-exchange resins; Sr resin) for Rb and K purification. We show that AMP-PAN resin and Sr resin can readily separate Rb from K and other matrix elements. However, AMP-PAN resin has a high Rb blank (~80 ng) and is cumbersome to use, which limits its applicability. For cation resins, we test the effects of column length, acid molarity, temperature, pressure drop (flow rate), and resin cross-linkage on the Rb separation using a Fluoropolymer Pneumatic Liquid Chromatography (FPLC) unit built in our laboratory. Increasing column length or resin cross-linkage has a positive effect on the separation, while increasing acid molarity, temperature, or pressure drop (flow rate) has negative impacts. Gravity-driven cation-exchange resin columns fail to cleanly separate Rb from K, but an AG50W-X12 resin column of 150 cm length and 0.16 cm inner diameter installed on a FPLC unit can cleanly separate Rb from K. We separated Rb from synthetic and natural rock samples using three different purification schemes designed based on the three types of resins, and measured the Rb isotopic compositions of the Rb separates by MC-ICPMS. The three methods yielded consistent results, demonstrating the efficacy of our Rb separation and the accuracy of our Rb isotopic analyses. The Rb isotopic compositions of several geostandards were analyzed (BCR-2, BHVO-2, BE-N, AGV-2, GS-N, G-3, and G-A), which can be used in future studies for ground-truthing methodologies used for studying natural samples. Among the three methods, the Sr resin method is the most straightforward for purifying Rb and K simultaneously, and measuring their isotopic compositions in natural samples.

Received 29th July 2021
Accepted 6th October 2021

DOI: 10.1039/d1ja00268f

rsc.li/jaas

1. Introduction

Alkali metals (Li, Na, K, Rb, Cs, and unstable Fr) are a group of elements that have found considerable use in geochemistry and cosmochemistry. They are univalent, redox insensitive, moderately volatile, lithophile, and fluid mobile. Among them, Li, K, and Rb have at least two stable or long-lived isotopes, and measurements of their isotopic ratios by multi-collector inductively coupled plasma mass spectrometry (MC-ICPMS) have provided new insights into geochemical processes such as volatile element depletion during planetary formation, continental crust extraction and recycling by subduction, and surface weathering and climate feedbacks (*e.g.*, ref. 1–21, and references therein).

A major obstacle to the routine isotopic analysis of these alkali elements by MC-ICPMS is the presence of potential isobaric interferences and matrix effects that can cause changes in instrumental mass-bias. It is therefore critical to purify the element of interest using ion exchange chromatography prior to isotopic analysis. Purifying Li and K is relatively straightforward (*e.g.*, ref. 2, 9, 11 and 22–24). However, purifying Rb from rocks for high-precision isotopic analyses is rather difficult, mostly because it is a trace element that follows K closely in aqueous chemistry. This is not a problem for K isotopic analysis because the weight K/Rb ratio in terrestrial rocks and meteorites ranges from ~50 to 1000,[25] so Rb does not need to be separated for K

[a]*Department of the Geophysical Sciences and Enrico Fermi Institute, The University of Chicago, Chicago, IL 60637, USA*

[b]*Earth and Planets Laboratory, Carnegie Institution for Science, Washington, DC 20015, USA. E-mail: nnie@carnegiescience.edu*

[c]*Department of Earth and Environment, Boston University, Boston, MA 02215, USA*

[d]*The Isotoparium, Division of Geological and Planetary Sciences, California Institute of Technology, Pasadena, CA 91125, USA*

isotopic analysis.[26] The opposite is not true, as precise Rb isotopic analysis by MC-ICPMS requires a K/Rb ratio of less than 10.[14] An additional challenge is that Rb has only two stable isotopes, ^{85}Rb and ^{87}Rb (with isotopic abundances of 72.17 and 27.83%, respectively), meaning that a double spike technique[27] cannot be used to correct for potential isotopic fractionation during chromatographic purification and MC-ICPMS analysis. A high Rb yield is therefore essential for minimizing isotopic fractionation during chromatography[28] and obtaining accurate Rb isotopic data.

Studies on Rb stable isotopes (*i.e.*, ^{87}Rb/^{85}Rb ratios) are so far very limited, despite its great potential for probing diverse geological and planetary processes. Waight *et al.*[29] used a Zr-doping method for the determination of Rb isotopic compositions by MC-ICPMS. Nebel *et al.*[30] applied this method to Rb-enriched natural samples such as mica and granites, and obtained a precision of $\sim\pm0.5‰$ on the ^{87}Rb/^{85}Rb ratio. Nebel *et al.*[6] measured chondrites using the same method and found no Rb isotopic variation among the samples within $\pm1‰$. Pringle and Moynier[12] used cation exchange chromatography to separate Rb from rock matrices but they reported no elution curve, and it is unclear whether Rb was efficiently separated from K in that study. They reported a precision of Rb MC-ICPMS analysis of $\sim\pm0.05‰$, and found small isotopic differences between terrestrial rocks, lunar samples, and chondrites, some of which have been replicated by Nie and Dauphas.[14] Zhang *et al.*[28] developed a Rb chromatography purification method using a single Sr resin column and applied it to several geostandards. Building on that work, Nie and Dauphas[14] achieved a cleaner separation of Rb from K and other matrix elements for study of Rb-depleted samples by using more elongated columns, and reported Rb isotopic analyses of lunar samples with precisions of $\sim\pm0.05‰$. Combining these data with K isotope data reported previously,[10] Nie and Dauphas[14] concluded that vapor drainage from the protolunar disk onto the Earth was the most likely cause for lunar volatile element depletion. Rubidium isotopic analysis may also find some applications in studies of surface weathering.[31,48] Almost all analyses of terrestrial samples so far have focused on geostandards and igneous rocks which have relatively abundant Rb,[12,14,28,30,48] and a reliable chemical purification method is required for the broader applications of Rb isotopes.

Three resins have been used in the literature for purifying Rb, including AMP-PAN resin,[32,33] cation-exchange resins,[6,12] and Sr resin.[14,28] In this work, we test the effectiveness of these three resins. We also develop three complete Rb separation procedures using the three resins, and apply them to synthetic and natural samples, which allow us to test the accuracy of the obtained Rb isotopic compositions through cross-comparison.

2. Materials and methods

2.1 Reagents and columns

Nitric (HNO_3) and hydrochloric (HCl) acids of analytical grade were double-distilled in a two-stage quartz-fluoropolymer sub-boiling distillation unit before use. High purity (99.999%) ammonium salts (ammonium nitrate and ammonium chloride) were used for making NH_4NO_3 and NH_4Cl solutions. Teflon labware was cleaned with water and aqua regia (concentrated acid mixture of 3 : 1 HCl and HNO_3 in volume) before use. Milli-Q water (18.2 MΩ cm at 25 °C) was used for diluting acids, dissolving ammonium salts, and cleaning. We used different empty columns for packing the ion exchange resins and testing the separation of Rb. These included disposable Bio-Rad 10 mL Poly-Prep columns and 20 mL Econo-Pac columns, perfluoroalkoxy alkane (PFA) columns from Savillex with inner diameter (ID) of 0.45 cm and customized lengths of 10–40 cm, and home-made PFA columns with 0.16 cm ID and various lengths of 70–150 cm (for using in the fluoropolymer pneumatic liquid chromatography (FPLC) system; see Sect. 2.3).

2.2 AMP-PAN resin

The AMP-PAN resin was purchased from Eichrom. The effective component of the AMP-PAN resin is Ammonium Molybdo-Phosphate (AMP), which is an inorganic ion exchanger with a microcrystalline structure. In the AMP-PAN resin, those microcrystallites are embedded in an organic matrix of polyacrylnitrile (PAN) to better control fluid flow and resin-fluid exchange. Ammonium heteropolyacid salts have long been known for their cation exchange properties for alkali metal ions.[34] Among them, AMP shows great potential in separating alkali metals.[32,33] The principle behind its use is the substitution of the large ammonium ion NH_4^+ in the AMP by large alkali metal cations. The larger the alkali ions, the easier the substitution. The AMP-PAN resin therefore has very high selectivity of Cs, and is primarily used for treating Cs-contaminated radioactive wastes.[35]

Because of the microcrystalline structure of AMP, early studies mixed fine crystals of AMP with asbestos to achieve favorable flow rates for column chromatography.[32] The AMP-PAN resin from Eichrom embeds AMP in PAN to control the particle size and porosity. Despite its potential in separating alkali metals, the AMP-PAN resin has not been systematically tested for this purpose. Here we test if the resin can be used to separate Rb from K for isotopic analysis.

In order to optimize chromatography separation schemes, it is useful to simulate expected elution curves on the basis of the theory of plate, which requires knowledge of partition coefficients of elements between the resin and eluent (*e.g.*, ref. 36 and 37). Because these are unknown for the AMP-PAN resin, we have determined the distribution coefficients for multiple selected elements (see Sect. 3.1).

2.3 Cation-exchange resins and the FPLC system

The cation-exchange resins (AG50W-X8 200–400 mesh and AG50W-X12 200–400 mesh; both in H^+ form) are available from Bio-Rad. Cation-exchange resins are among the most commonly used resins for elemental purification in analytical chemistry, and distribution coefficients between cation-exchange resins and acids are well known. A complete set of distribution coefficients of elements in HCl, HNO_3 and H_2SO_4 media on the cation resin AG50W-X8 have been previously determined.[38,39] Some of previous Rb isotope studies used cation resins[6,12,30] and

diluted HCl to separate Rb from matrix elements, but no elution curves were reported. Nie and Dauphas[14] did a preliminary test on the Rb separation with AG50W-X8 200–400 mesh resin using a short column (1 mL column of 0.6 cm ID and 3.5 cm length), and showed significant overlap between Rb and K peaks during elution, calling for further refinements.

Several factors can contribute to the efficiency of a chromatography column, including the resin properties (*i.e.*, resin mesh size, cross-linkage, nature of the cation), the dimension of the column (*i.e.*, column length and inner diameter), the nature (*i.e.*, acid type and molarity) and velocity (flow rate) of the liquid eluent, and temperature. For a given volume of resin, it is preferable to use longer (thinner) columns as higher resolution is achievable. Columns that are relatively long and thin are difficult to run by gravity, but this issue can be mitigated by applying a pressure differential between the column top and bottom. In this work, we explore how the pressure drop (*i.e.*, the pressure difference between the column head and the outlet, which is directly related to flow rate), the length of the column, acid molarity, cation resin cross-linkage, and temperature affect Rb purification, with the goal of finding a method that efficiently separates Rb from K using only cation resins. Those tests include elution columns that are extremely long (70 to 150 cm in length) and thin (0.16 cm ID), run under different pressure drops and at different temperatures. In order to perform these tests, we used a FPLC system that was designed, developed, and

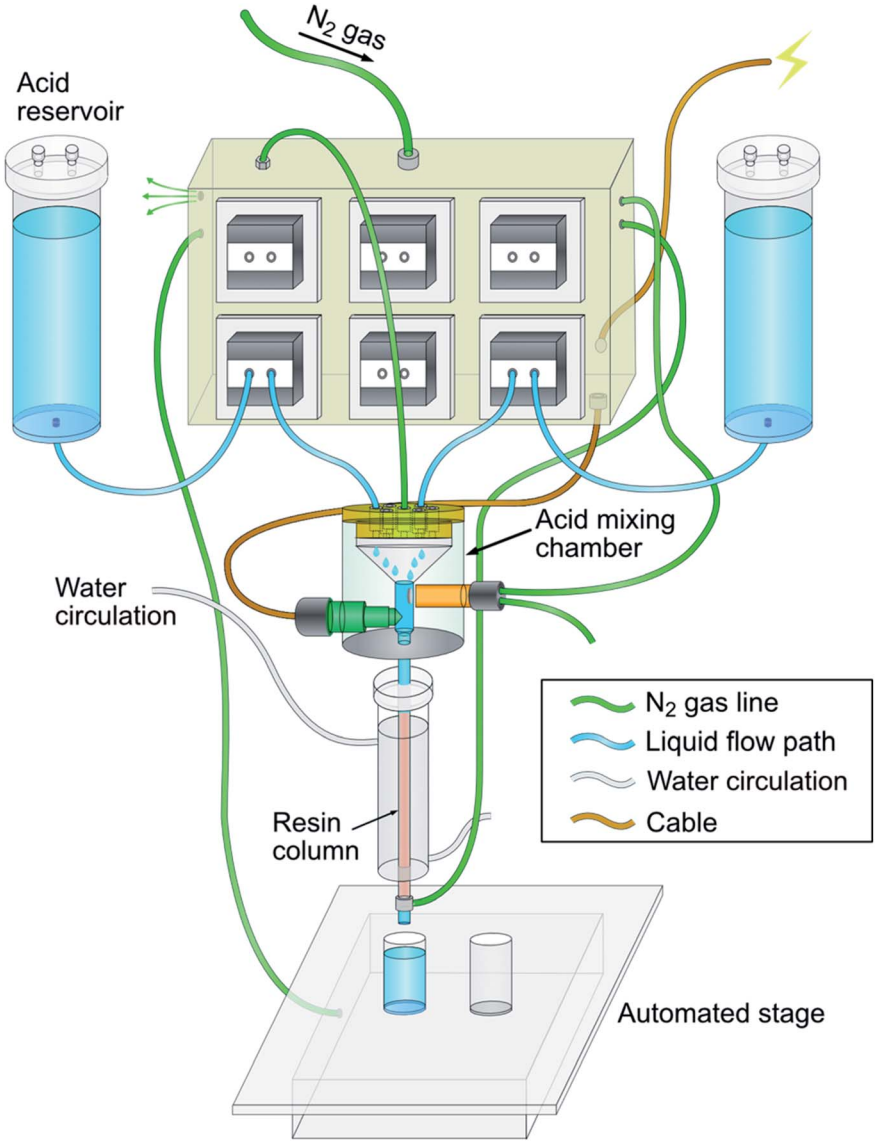

Fig. 1 The sketch of the fluoropolymer pneumatic liquid chromatography (FPLC) system. The major components of the system include acid reservoirs (filled with acids in different molarities and Milli-Q water), acid mixing chamber (to obtain acids in different molarities by mixing reservoir acids with Milli-Q water), the resin column, and the stage that is automatically movable for collecting eluates in different vials. The system is automated and computer-controlled using a LabView software interface. Elution pressure is adjustable (from 0 to 70 psi, *i.e.*, 4.8 bar) by pressurizing high-purity N_2 gas to force the eluents through the column, and elution temperature is adjustable (from 0 to 80 °C) through a water circulation system.

built in the Origins Lab at the University of Chicago.[36,40,41] A sketch of the FPLC system is shown in Fig. 1.

The FPLC system used in the present study is an updated version of the system described in ref. 36 that has been used most recently for separating rare earth elements,[41] which are difficult to be separated from each other due to their similar chemical behaviors. There are several distinctive features about the FPLC unit that allow unprecedented separation of elements with similar behaviors: (i) column elution is automated and computer-controlled using a LabView software interface, allowing the use of very long/thin columns that may take long elution time, (ii) the liquid flow path is made of fluoropolymer that has a high acid resistance and a low alkali element blank, (iii) the elution temperature is controlled by a water circulation system, and can be adjusted from room temperature to 80 °C, and (iv) it uses high-purity N_2 gas to force the eluents through the column, and the extra pressure imposed on the column head can be adjusted from 0 to 70 psi (~4.8 bar) to achieve a desired flow rate.

2.4 Sr resin

The Sr resin is commercially available from Eichrom. The Sr resin is composed of 4,4′(5′)-di-*t*-butylcyclohexano-18-crown-6 (crown ether) in 1-octanol. The distribution coefficients of elements including alkalis in HNO_3 medium have been characterized by Horwitz *et al.*[42] The distribution coefficients of alkali elements on the Sr resin are generally moderate or low (less than 10), with K partitioning more strongly in the resin than Rb. According to the distribution coefficients, the largest separation between K and Rb (*i.e.*, the largest relative difference between their distribution coefficients) occurs at ~2–3 M HNO_3. Following previous work on Rb separation,[14,28] we use 3 M HNO_3 as the sample loading medium and the eluent. We tested three lengths of Sr columns (13, 20, and 40 cm) with an ID of 0.45 cm. A vacuum box from Eichrom was used to increase the flow rate.

2.5 Mass spectrometry

Element concentrations were determined using the MC-ICPMS in the Origins Lab at the University of Chicago. Multi-element solutions were prepared with elements in equal concentrations of 100 μg g^{-1} by mixing single-element standard solutions. The multi-element solutions were diluted as needed for loading onto the columns and for using as elemental standards during concentration measurements. Elution aliquots were introduced into the MC-ICPMS *via* a dual cyclonic-Scott-type quartz spray chamber at a flow rate of ~100 μL min^{-1}. Peak jumping was used for measuring the concentrations of the multiple elements in each solution aliquot, and each element was measured for 5 cycles of 4.194 s integration time, with an idle time of 3 s between two different elements. Every batch of three samples was bracketed by two standards, and the concentrations were calculated by comparing the intensities of samples with the time-interpolated intensity averages of the two bracketing standards.

Measurements of Rb isotopic compositions of purified Rb solutions by MC-ICPMS followed the general method used in ref. 14. Nie and Dauphas[14] used 15–25 ng g^{-1} Rb solution for measurements as limited amount of Rb was available in lunar samples, while we used here concentrations of ~100 ng g^{-1} as we are not limited by the Rb amount in the selected terrestrial samples. It is always preferred to use a more concentrated solution to increase the signal/noise ratio. Rubidium was measured in wet plasma mode and was introduced into the MC-ICMPS using a dual cyclonic-Scott-type quartz spray chamber at a flow rate of ~100 μL min^{-1}, yielding an ^{85}Rb signal of ~5 V or higher on a 100 ng g^{-1} solution. The major interference on Rb isotopes is isobaric $^{87}Sr^+$ on $^{87}Rb^+$, which cannot be resolved using even the high-resolution slit. A low-resolution slit was therefore used for Rb isotopic analysis, but attention was paid to monitoring the amount of Sr present in the purified Rb solution by measuring the intensity of ^{88}Sr. For all the measurements reported here, an $^{88}Sr^+/^{85}Rb^+$ intensity ratio below 5×10^{-4} was achieved after Rb purification, and using the measured ^{88}Sr and assuming an $^{87}Sr/^{88}Sr$ of 0.085 were sufficient to accurately correct for ^{87}Sr interference. Each data was collected as a single block of 25 cycles of 4.194 s integration time. Standard-sample bracketing was used to correct for instrumental mass-bias. Each sample (bracketed by standard) was measured 7–10 times, the mean $\delta^{87}Rb$ value was taken, and the uncertainty was calculated as 95% confidence interval (c.i.) using the formula $2\sigma/\sqrt{n}$, where n is the number of replicates of a sample and σ the standard deviation of the $\delta^{87}Rb$ of the standard bracketed by itself in an entire session (~10 hours). The σ was quantified using the standard instead of the sample because the standard was measured many more times (several different samples were measured in one session and they were all bracketed by the same standard), so the standard deviation is better quantified. All Rb isotopic compositions are reported as $\delta^{87}Rb$ values, which are the per mil deviation of the $^{87}Rb/^{85}Rb$ ratios of the samples from that of the Rb reference standard NIST SRM984.

3. Results

3.1 Rubidium purification using AMP-PAN resin

The distribution coefficients of a group of selected elements on the AMP-PAN resin were determined. The distribution coefficient (K_d) describes the partitioning of an element between the solid resin and the liquid eluent at equilibrium,

$$\text{Distribution coefficient } (K_d) = \frac{C_i^{\text{resin}} \text{ per gram resin}}{C_i^{\text{solution}} \text{ per mL solution}}, \quad (1)$$

where C_i^{resin} is the concentration of an element i partitioned into the resin (in mg g^{-1} dry resin), and C_i^{solution} is the concentration of the element in the liquid phase (in mg mL^{-1} solution). It is not straightforward to determine the elemental concentration in the resin, therefore, a modified form of eqn (1) was used to calculate the distribution coefficient of an element that relies solely on solution concentration measurements,

$$\text{Distribution coefficient } (K_d) = \frac{V\left(C_{i,0}^{\text{solution}} - C_i^{\text{solution}}\right)}{WC_i^{\text{solution}}}, \quad (2)$$

where $C_{i,0}^{solution}$ and $C_{i}^{solution}$ are the elemental concentrations in the liquid solution in mg mL^{-1} before and after equilibration, respectively. V is the volume of the solution (in mL), and W is the weight of dry resin (in g).

Ammonium solutions have to be used to recover alkali elements from AMP-PAN resin, which involved the substitution of high-affinity NH_4^+ for K^+ and Rb^+. Therefore, we determined the distribution coefficients of elements in both HNO_3 and NH_4NO_3 solutions. A potential advantage of using HNO_3 and NH_4NO_3 to determine the distribution coefficients, compared to HCl and NH_4Cl, is that NH_4NO_3 has a higher solubility in water compared to NH_4Cl (1.5 g mL^{-1} H_2O for NH_4NO_3 *vs.* ~0.4 g mL^{-1} H_2O for NH_4Cl at room temperature), thus allowing for a more concentrated ammonium solution. Nevertheless, we also ran some tests with HCl and NH_4Cl, bearing in mind that anions NO_3^- and Cl^- should not influence much the distribution coefficients as NH_4^+ is the main driver.

In preparation for batch equilibration experiments, a multi-element solution containing alkali metals Na, K, Rb, and Cs together with several other major and trace elements (Ti, Al, Mg, Ca, Sr, U, Fe, Zn) was prepared, by mixing single-element standard solutions in equal concentrations. Aliquots of the multi-element solution were transferred to PFA beakers, dried on a hotplate and re-dissolved in HNO_3 or NH_4NO_3 solutions in different molarities. The molarities of the final solutions used for the batch equilibration experiments were 0.1, 1, 2, 4, 6, 8 and 10 mol L^{-1} for HNO_3, and 0.01, 0.1, 1, 2, 4, 6, 8 and 10 mol L^{-1} for NH_4NO_3 solutions. Each solution was added to a centrifuge tube containing ~200 mg of the dry resin for equilibration and was shaken manually every 2 hours. After ~8 hours of equilibration, the mixtures were filtered using empty Bio-Rad Poly-Prep columns to separate the liquid from the resin. The solutions were collected in PFA beakers and diluted using 0.3 M HNO_3 for concentration analysis by MC-ICPMS.

The distribution coefficients (K_d) of elements on AMP-PAN resin as a function of HNO_3 and NH_4NO_3 molarity are shown in Fig. 2, in base-10 logarithmic scale. The higher the distribution coefficient, the more strongly the element is bound to the resin and the larger eluent volume is needed to elute the element. The most salient results of our determination of the distribution coefficients are, (i) non-alkali elements have relatively low distribution coefficients in both HNO_3 and NH_4NO_3 solutions, in general less that 10, suggesting that they can be released from the resin; (ii) alkali metals Na, K, Rb, and Cs have increasingly higher distribution coefficients as a function of ion size in both HNO_3 and NH_4NO_3 solutions; Rb and Cs in particular have much higher distribution coefficients than other elements, suggesting that they can be strongly fixed onto the resin; (iii) differences between distribution coefficients of alkali metals at a similar HNO_3/NH_4NO_3 molarity are large, implying that they can be efficiently separated from each other, and (iv) the distribution coefficient of Rb is very high in HNO_3 (100–1000) but is decreased in NH_4NO_3 solutions (Fig. 2), meaning that NHO_3 and NH_4NO_3 can potentially be used as the loading medium for fixing Rb onto the resin and the eluent for recovering Rb, respectively.

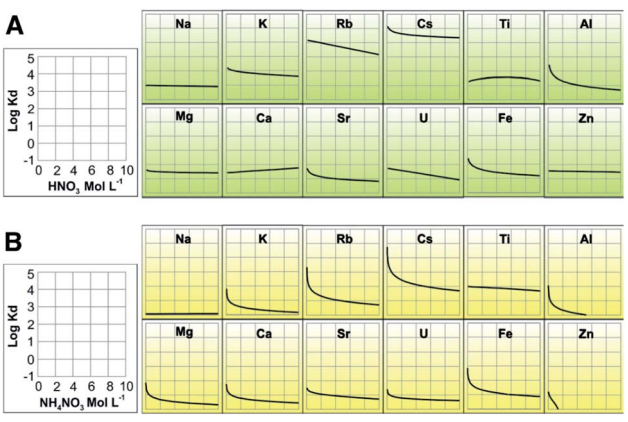

Fig. 2 Distribution coefficients (K_d) in base-10 logarithmic scale of alkali metal elements and several other elements on AMP-PAN resin, as a function of (A) HNO_3 molarity, and (B) NH_4NO_3 molarity.

Given the high distribution coefficient of Rb in HNO_3 and low distribution coefficient of Rb in NH_4NO_3 (Fig. 2), the expectation is that a small column would be sufficient to separate Rb from other elements. Therefore, the resin columns used for testing the AMP-PAN resin have a 1 mL resin bed (0.8 cm ID and 2 cm length) in Bio-Rad Poly-Prep empty columns. The tests were done first by loading 500 μL of a multi-element solution (20 μg g^{-1} of each element) onto the column in 4 M HNO_3, followed by 15 mL 4 M HNO_3 to elute matrix elements and K, and then 20 mL 4 M NH_4NO_3 to recover Rb (Fig. 3A). Solutions passed through the column were collected in 1 mL steps. The elution curves are shown in Fig. 3A. For easier comparison, *y*-axis of all elution curves in this study is normalized intensity, and the total area below an elution curve would be 1 for 100% recovery of the element. The elution curves reveal that: (i) matrix elements (*e.g.*, Na, Mg, Al, Ca, Fe, Ti) are not bound to the resin and are effectively eluted with 4 M HNO_3, as expected from their low distribution coefficients (Fig. 2), while Rb is strongly fixed to the resin, and (ii) Rb can be eluted in 4 M NH_4NO_3.

Several problems were, however, noticed during the elution. The first problem is that during the elution of Rb with 4 M NH_4NO_3, significant amount of K is also eluted (Fig. 3A). The amount of K eluted previously by HNO_3 is about the same amount as that was loaded onto the column, so K is not expected during Rb elution with NH_4NO_3. The high K signal during NH_4NO_3 elution of Rb is likely caused by K impurities in the NH_4NO_3 solution. This is supported by the relatively constant K concentration among all cuts eluted with 4 M NH_4NO_3 solution (Fig. 3A). Secondly, we also observed during the tests that the resin was partially dissolved in the NH_4NO_3 solution. After passing through the column, the NH_4NO_3 solution that contains eluted Rb is clear initially, but small yellow particles form upon heating that could not be re-dissolved. In addition, large amounts of phosphorus and Mo from dissolved AMP are present together with Rb in NH_4NO_3, and they have to be removed before Rb analysis, which requires further purification steps. Converting the eluted Rb from NH_4NO_3 solution to HNO_3 solution is difficult because the decomposition of

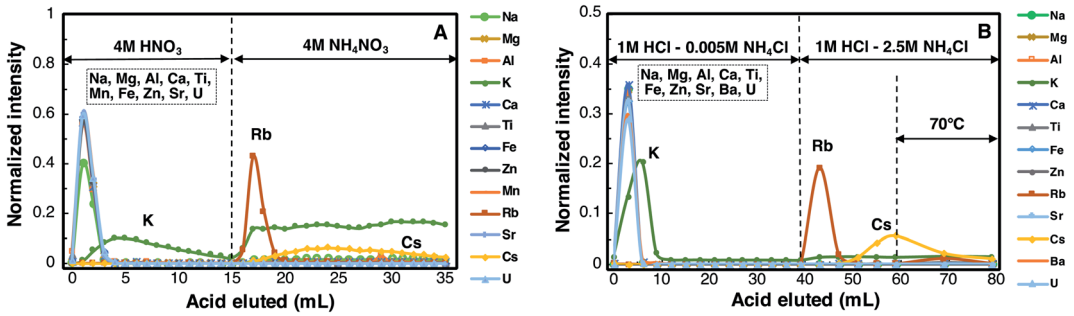

Fig. 3 Elution curves of elements on AMP-PAN resin. (A) Elution using HNO_3 and NH_4NO_3. Several problems have been observed for this elution scheme, including resin decomposition during elution, high K blank in NH_4NO_3, and difficulties in follow-up treatment of the Rb in NH_4NO_3 eluate (see Sect. 3.1 for details). (B) Purification of Rb with AMP-PAN resin using HCl and NH_4Cl. Rubidium was eluted in two steps. A solution of 1 M HCl–2.5 M NH_4Cl was first passed through the resin to collect Rb (~70–80% of the total Rb was recovered), and the remaining Rb was recovered by two 10 mL batch extraction steps at 70 °C (>95% Rb was recovered after this step).

NH_4NO_3 by heating can be potentially hazardous since it is a strong oxidizer, and the decomposition reaction is exothermic, which can lead to a runaway reaction under certain conditions.

To circumvent the problems associated with NH_4NO_3, we additionally tested an elution scheme using HCl and NH_4Cl solutions (Fig. 3B). We lowered the concentration of NH_4Cl to 2.5 M to decrease the K background. For washing out K and matrix elements, we used a mixture of dilute HCl (1 M) and NH_4Cl (0.005 M). For eluting Rb, we used a solution of 1 M HCl–2.5 M NH_4Cl. A HCl–NH_4Cl mixture instead of a pure NH_4Cl solution was used because the yield of Rb was higher (~80%) with the former than with the latter (~60%). The quite low Rb yield in pure ammonium solutions on the AMP-PAN resin (~60%) is likely caused by partial blocking of the channels in the AMP crystal lattice after Rb fixation (personal communication with Dr Šebesta who developed the AMP-PAN resin). A solution to this problem is to use a mixture of HCl–NH_4Cl solution for Rb elution, and then to add an additional 10 mL of the 1 M HCl–2.5 M NH_4Cl mixture to the column and place it in the oven at 70 °C for batch equilibrium for 2–3 hours, and to repeat this batch equilibration step a second time (Fig. 3B). This treatment partially decomposes the AMP resin and the Rb yield after this treatment is >95%. While particle formation was observed in the chemistry involving NH_4NO_3 solution, no such phenomenon was observed in NH_4Cl elution. This could be because a less concentrated NH_4Cl solution was used (2.5 M NH_4Cl *vs.* 4 M NH_4NO_3), and/or the possibility that AMP-PAN is more affected by NO_3^-. A virtue of using NH_4Cl is that it is not as hazardous as NH_4NO_3 and decomposes into NH_3 and HCl gases upon heating at a temperature of ~338 °C. In our tests, NH_4Cl was removed from the eluate solution containing the recovered Rb by a two-step heating process: (i) the solution was transferred to a Pt crucible (pre-cleaned with double distilled HCl), and evaporated to dryness on a hotplate at a temperature of ~90 °C (at this point NH_4Cl appears as a white solid), and (ii) the temperature was slowly increased (to avoid boil over) to around 350 °C on the hotplate, and was held there until all NH_4Cl decomposed and no white residue was left. Rubidium left in the Pt crucible was then dissolved in nitric or hydrochloric acid solutions for further treatment.

The AMP-PAN resin releases large amounts of NH_4^+, Mo, and P in the Rb eluate. Although NH_4^+ may be removed (and possibly P as well, given that P_2O_5 melts and sublimes at ~350 °C) during heating of the solution to 350 °C, Mo has to be removed using another resin column. We removed Mo using a 1 mL column (0.8 cm ID and 2 cm length) of 200–400 mesh anion-exchange resin AG1-X8. The complete procedure for extracting Rb using AMP-PAN resin is summarized in Table 1. The Rb blank of the procedure including the elution and the following treatment is ~80 ng. We did not consider separating K using the AMP-PAN resin because of the high K background in the ammonium solutions (Fig. 3) and the fact that there are far better alternatives.

3.2 Rubidium and potassium purification using cation-exchange resins

We performed a series of tests on cation resins, evaluating how resin cross-linkage, acid molarity, column length, pressure drop (flow rate), and temperature affect the separation of Rb and K (Table 2 and Fig. 4–6). The columns used here include both gravity-driven short columns (1.5 cm ID, 6.8 or 9 cm length, and 0.45 cm ID and 20 cm length; Fig. 4), and columns that are extremely long and thin (0.16 cm ID and 70–150 cm in length; Fig. 5 and 6), which were run using the FPLC system and took about 10–40 hours for one elution depending on the length and the pressure drop. For gravity-driven columns, about 500 μL multi-element solutions (at a concentration for all elements of ~20 μg g^{-1}) were loaded onto columns in 0.5 M HNO_3, and for the FPLC columns, about 200 μL multi-element solutions were loaded in 0.1 M HNO_3. The elution of elements was done using 0.5–1 M HNO_3. A lower acid molarity is associated with a higher distribution coefficient for cation resins,[38,39] and thus requires a larger amount of eluent. At higher acid molarity, however, the Rb and K elution peaks are less resolved. We used HNO_3 for the elution instead of HCl because the solutions can be directly diluted for MC-ICPMS analyses of concentrations (HCl is usually avoided as it produces a wider array of isobaric interferences), but HNO_3 and HCl should yield similar results for cation resins, as the exchanging species of the resin is H^+.

Table 1 Elution sequences of the three Rb purification procedures

Separation steps	Reagents	Volume (mL)	Comments
(1) AMP-PAN resin method			
Column 1, AMP-PAN resin, 1 mL resin (0.8 cm ID, 2 cm length) in Bio-Rad Poly-Prep columns			
Conditioning	1 M HCl–0.005 M NH_4Cl	2	
Sample loading	1 M HCl–0.005 M NH_4Cl	0.1	
Elution of K and matrix elements	1 M HCl–0.005 M NH_4Cl	20	
Elution of Rb	1 M HCl–1 M NH_4Cl	20	
Further recovery of Rb from resin	1 M HCl–2.5 M NH_4Cl	10	Batch extraction at 70 °C
Further recovery of Rb from resin	1 M HCl–2.5 M NH_4Cl	10	Batch extraction at 70 °C
Combine and dry the recovered Rb solutions in Pt crucible at 350 °C			Removal of NH_4Cl
Column 2, AG1-X8 resin, 200–400 mesh, 1 mL resin (0.8 cm ID, 2 cm length) in Bio-Rad Poly-Prep columns			For Mo removal
Conditioning	5 M HCl–H_2O_2	2	H_2O_2/HCl = 0.5% (v/v)
Sample loading	5 M HCl–H_2O_2	1	H_2O_2/HCl = 0.5% (v/v)
Elution of Rb	5 M HCl	9	Mo stays on the column
(2) Cation-exchange resins + FPLC method			
Column 1, AG50W-X8 resin, 200–400 mesh, 16 mL resin (1.5 cm ID, 9 cm length) in Bio-Rad Econo-Pac columns			
Conditioning	0.5 M HNO_3	16	
Sample loading	0.5 M HNO_3	≤8	
Elution of matrix	0.5 M HNO_3	130	
Elution of Rb and K	0.5 M HNO_3	350[a]	Contains some Ti
Column 2, AG1-X8 resin, 200–400 mesh, 1 mL resin (0.8 cm ID, 2 cm length) in Bio-Rad Poly-Prep columns			For Ti removal
Conditioning	2 M HF	2	
Sample loading	2 M HF	0.25	
Elution of Rb and K	2 M HF	9	Ti stays on the column
Column 3, AG50W-X12 resin, 200–400 mesh, home-made column of 0.16 cm ID and 150 cm length on FPLC			Elution at pressure drop of 60 psi
Conditioning	0.1 M HNO_3	10	(linear flow rate of ~3 cm min^{-1})
Sample loading	0.1 M HNO_3	0.2	
Elution of K	0.7 M HNO_3	~85[b]	
Elution of Rb	0.7 M HNO_3	~35[b]	
(3) Sr resin method			
Column 1, AG50W-X8 resin, 200–400 mesh, 16 mL resin (1.5 cm ID, 9 cm length) in Bio-Rad Econo-Pac columns			
Conditioning	0.5 M HNO_3	16	
Sample loading	0.5 M HNO_3	≤8	
Elution of matrix	0.5 M HNO_3	130	
Elution of K and Rb	0.5 M HNO_3	350[a]	Contains some Ti
Column 2, AG1-X8 resin, 200–400 mesh, 1 mL resin (0.8 cm ID, 2 cm length) in Bio-Rad Poly-Prep columns			For Ti removal
Conditioning	2 M HF	2	
Sample loading	2 M HF	0.25	
Elution of Rb and K	2 M HF	9	Ti stays on the column
Column 3, Sr resin, 50–100 μm size, in Savillex columns of 0.45 cm ID and 40 cm length			Elution at pressure drop of 2.5 psi
Conditioning	3 M HNO_3	5	(linear flow rate of ~0.8 cm min^{-1})
Sample loading	3 M HNO_3	0.1	
Elution of matrix	3 M HNO_3	3.9	
Elution of Rb	3 M HNO_3	12	
Elution of K	3 M HNO_3	20	

[a] The 350 mL eluate solutions were collected using Savillex PFA jars of 360 mL volume, dried on a hotplate at 130 °C, and re-dissolved in HF for the following step. [b] Eluate was collected every 1 mL between 80 and 90 mL elution, and Rb and K concentrations were measured in each collected volume to decide on the cutoff between Rb and K peaks. The collected volumes were then consolidated into K and Rb solutions. ID: inner diameter. v/v: volume/volume.

The elution curves are shown in Fig. 4–6. Fig. 4 shows the test results of gravity-driven columns of cation resin AG50W-X8 (200–400 mesh), one of the most commonly used cation resins, with column lengths varying from 6.8 to 20 cm (Fig. 4A–C). The effect of pressure drop between column top and bottom was tested using a vacuum box that is commercially available from Eichrom, by setting the pressure drop to 5 psi (~0.3 bar; Fig. 4D). Fig. 5 shows test results of the same cation resin, but using longer columns (column length ranging 70–120 cm), for which the FPLC system was used to pressurize the column head to achieve a reasonable flow rate. Fig. 6 shows the test results for a higher cross-linkage cation resin AG50W-X12 (200–400 mesh) for column lengths of 130 and 150 cm.

Overall, these elution tests show that: (i) alkali metals (together with Mo and Ti) are eluted out first from the resin by diluted HNO_3 (ranging from 0.5–1 M in our tests), while major elements such as Fe, Mg, Al, and Ca are bound to the resin until more concentrated acids (6 M HNO_3 or 6 M HCl) are used.

Table 2 Conditions of the elutions using cation-exchange resins

Elution	Resin type	Column length (cm)	Column ID (cm)	Temperature (°C)	Pressure drop[a] (psi)	HNO_3 molarity	Linear flow rate (cm min^{-1})	Number of plates[b]	Height of plate (cm)	Resolution[c]
Fig. 3A	AG50W-X8	6.8	1.5	20	0	0.5	0.50	232	0.03	0.68
Fig. 3B	AG50W-X8	9	1.5	20	0	0.5	0.46	322	0.03	0.87
Fig. 3C	AG50W-X8	20	0.45	20	0	0.5	0.27	360	0.06	0.99
Fig. 3D	AG50W-X8	20	0.45	20	5	0.5	2.11	56	0.36	0.43
Fig. 4A	AG50W-X8	70	0.16	20	30	0.5	4.61	280	0.25	0.61
Fig. 4B	AG50W-X8	70	0.16	20	60	0.5	8.30	185	0.38	0.39
Fig. 4C	AG50W-X8	120	0.16	20	60	0.5	4.00	357	0.34	0.88
Fig. 4D	AG50W-X8	120	0.16	20	60	1	3.91	549	0.22	0.88
Fig. 5A	AG50W-X12	130	0.16	20	60	0.8	2.99	902	0.14	1.64
Fig. 5B	AG50W-X12	130	0.16	70	60	0.8	5.72	507	0.26	0.65
Fig. 5C	AG50W-X12	150	0.16	20	60	0.7	2.93	1007	0.15	1.91
Fig. 5D	AG50W-X12	150	0.16	20	60	1	3.21	466	0.32	1.05

[a] Pressure drop is in psi. 5, 30 and 60 psi are equivalent to ~0.34, 2.06 and 4.14 bar, respectively. [b] Number of plates is estimated based on Rb peaks using $N = 16(D/w)^2$, where D is the volume corresponding to the elution of the Rb peak and w is the width of the Rb peak. [c] Resolution is calculated based on the separation between Rb and K peaks.

Therefore, alkali metals can be efficiently separated from other elements using cation resins, and (ii) column length, acid molarity, pressure drop (flow rate), temperature, and resin cross-linkage all influence cation resin elution. The effects of these parameters are discussed below. An important yet confounding factor, however, is flow rate. According to the theory of plates of chromatography,[43] slow flow rates result in smaller plate heights and better separations. However, if the flow rate is too low, vertical diffusion in the fluid becomes important, which can cause the height of the plate to increase.[44] We did not observe this diffusion effect for the columns in this study (*i.e.*, our observation is that a lower flow rate seems always to be associated with a better separation), meaning that even at the lowest flow rate studied, we are not in a regime where vertical diffusion matters. Flow rate, however, is not only dependent on pressure drop, but can change depending on column geometry

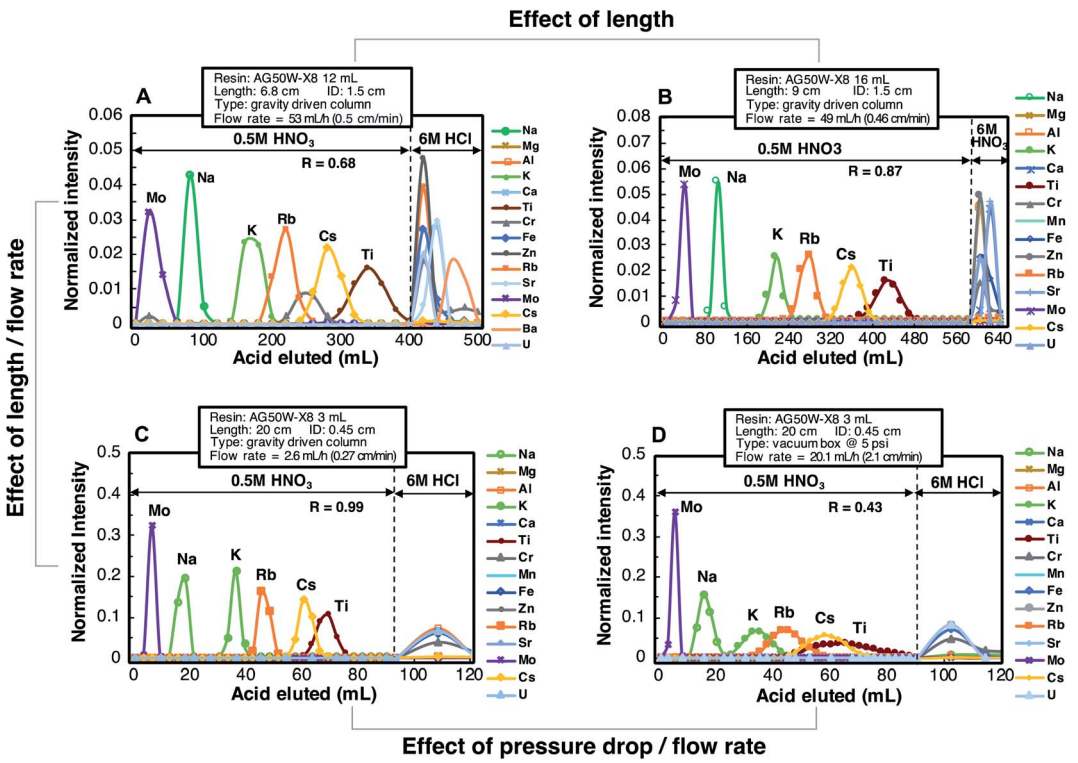

Fig. 4 Elution curves of gravity-driven AG50W-X8 (200–400 mesh) resin columns and of a column under slight pressurization (pressure drop of 5 psi or ~0.3 bar). Different lengths were tested. The R values in the figures denote the resolution between Rb and K peaks. Panel B is modified from ref. 14.

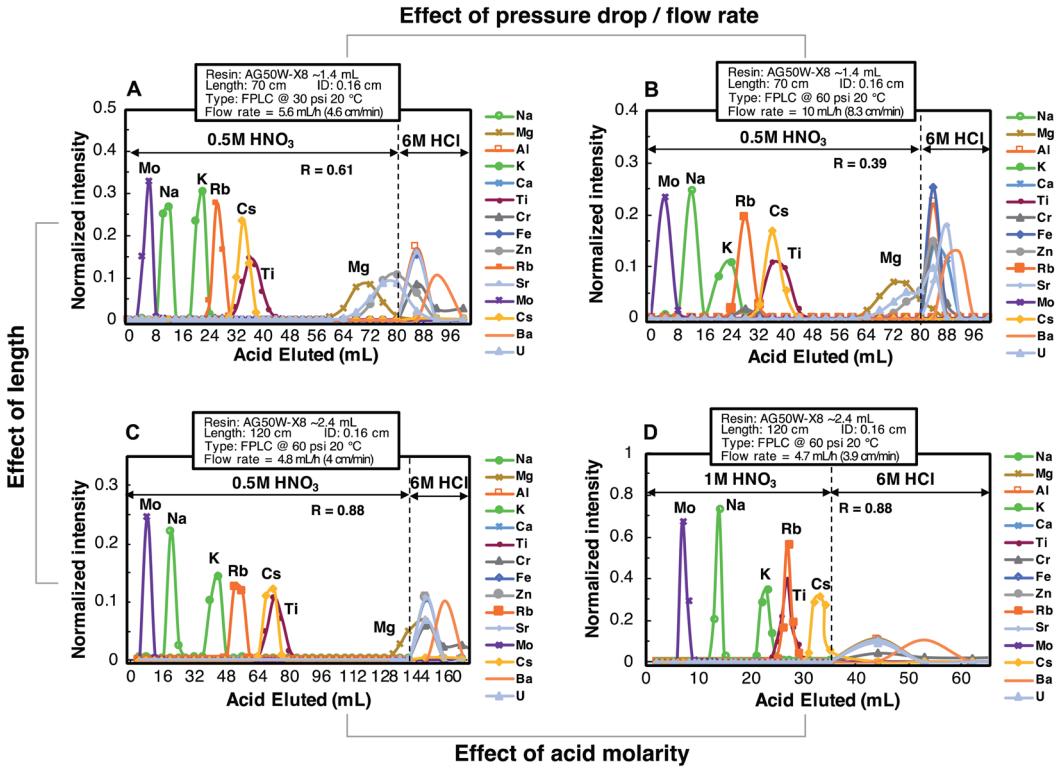

Fig. 5 Elution curves of AG50W-X8 (200–400 mesh) resin columns, obtained at different pressure drops (flow rates), column lengths, and acid molarities using the FPLC system.

(length and ID), resin cross-linkage, acid molarity, and temperature. In this study, we did not fully disentangle the effects of flow rate from other parameters, as our final goal was to find an elution scheme that separates Rb, so we focused on those variables that can be explicitly monitored and controlled (*e.g.*, temperature and pressure drop). Nevertheless, the flow rate associated with each elution is also reported.

For the elution curves, we use resolution R to define how well two peaks are resolved. The resolution R is expressed as,[45]

$$R = \frac{2d}{w_1 + w_2}, \quad (3)$$

where d is the separation between two peaks, and w_1 and w_2 the widths of the two peaks (*i.e.*, the distance between the points of intersection of the tangents to the inflection points with the base line), and we use the Rb and K peaks in the elution curves to calculate R. d and w are defined in the same unit of mL, so that R is dimensionless. Complete separation of the two peaks is considered to be achieved when $R > 1$. We also estimate the number of plates (Table 2) based on the Rb elution peak using,[45]

$$N = 16(D/w)^2 = 5.54(D/w_{0.5})^2, \quad (4)$$

where D is the volume of the Rb peak maximum, and w and $w_{0.5}$ are the width and the width at half height of the Rb peak, respectively. The plate height HETP can then be calculated from N and the length of the column L,

$$\mathrm{HETP} = L/N. \quad (5)$$

The values of N and HETP of the elutions, together with the elution conditions are summarized in Table 2.

Column length. According to the theory of plates for chromatography,[43] longer columns should result in better resolved peaks due to the larger number of theoretical plates. This is clearly observed in our tests of gravity-driven elutions (Fig. 4A–C and Table 2). The gravity-driven AG50W-X8 columns with different lengths of 6.8, 9, and 20 cm (Fig. 4A–C) show a decreasing overlap between elemental peaks (R increasing from 0.68 to 0.87 to 0.99; corresponding linear flow rates are 0.5, 0.46, and 0.27 cm min^{-1}, respectively). Although distinguishing the effects between column length and flow rate is difficult, comparing Fig. 4A and B demonstrates that column length is most likely the dominant factor as the flow rates are very similar (0.5 *vs.* 0.46 cm min^{-1}).

AG50W-X8 columns longer than 20 cm were tested using the FPLC system (Fig. 5). We measured elution curves produced by high-pressure (pressure drops of 30 and 60 psi, *i.e.*, ~2.1 and 4.1 bar, respectively) FPLC columns with lengths of 70 cm and 120 cm (Fig. 5A–C). The result shows that the 120 cm column yields a better separation (R = 0.88; flow rate = 4 cm min^{-1}) than the 70 cm column (R = 0.61) with a similar flow rate of 4.6 cm min^{-1}. For AG50W-X12 columns, a very similar flow rate was achieved for a 130 and a 150 cm column (Fig. 6A and C), and the 150 cm column shows a better separation (R = 1.91 *vs.* 1.64). However, this could also be partly due to the slightly different acid molarity used for the two columns (0.8 M HNO_3 *vs.* 0.7 M HNO_3).

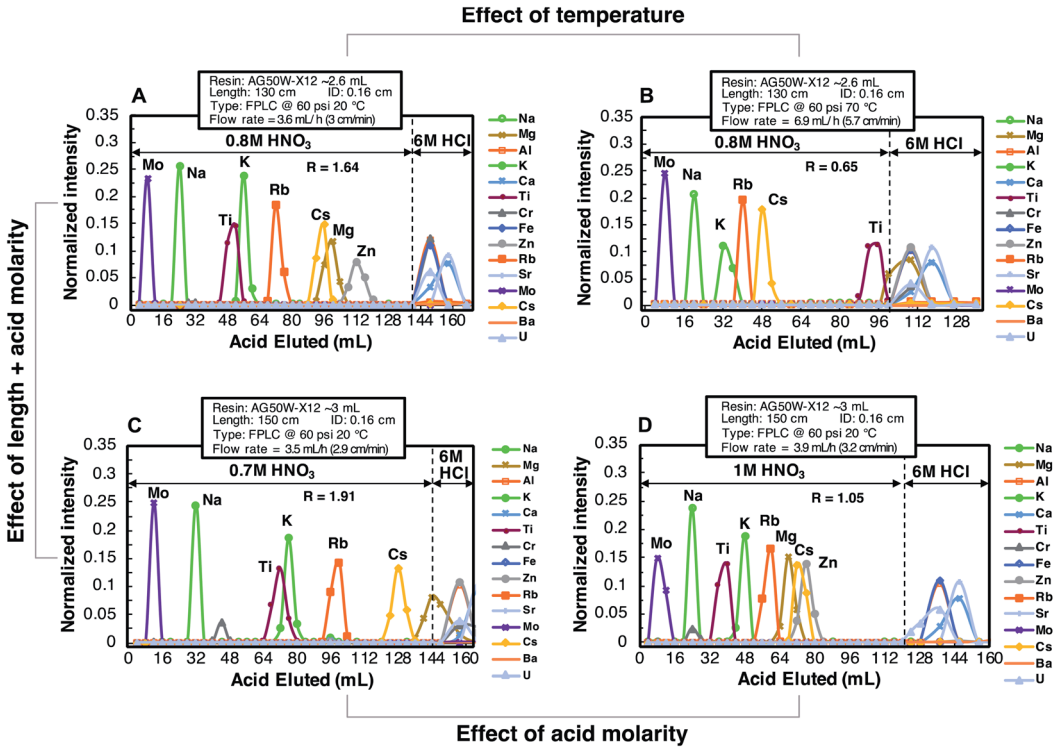

Fig. 6 Elution curves of AG50W-X12 (200–400 mesh) resin columns tested at different temperatures, column lengths, and acid molarities using the FPLC system.

Pressure drop (flow rate). Pressure drop directly controls flow rate. The effect of pressure drop was tested first on short AG50W-X8 columns (Fig. 4C and D). The pressure drop was created by using a vacuum box and was set to be 5 psi (~0.3 bar) (Fig. 4D). Comparing the gravity-driven separation and vacuum box separation using 20 cm-long columns (Fig. 4C and D) shows that the elevated pressure and flow rate (2.1 cm min^{-1}) lead to wider peaks that overlap significantly with each other ($R = 0.39$) compared to the ambient pressure ($R = 0.99$; flow rate = 0.27 cm min^{-1}).

We also tested the pressure drop on the FPLC long columns. A 70 cm-long column filled with AG50W-X8 resin was run at 30 psi (~2.1 bar; flow rate of 4.6 cm min^{-1}) and 60 psi (~4.1 bar; flow rate of 8.3 cm min^{-1}), respectively (Fig. 5A and B), resulted in a larger overlap between Rb and K peaks ($R = 0.39$) at 60 psi than at 30 psi ($R = 0.62$). This suggests again that a higher pressure drop (flow rate) has a negative effect on the separation. Nonetheless, the use of 60 psi is still advantageous because the flow rate was almost doubled compared to 30 psi (*i.e.*, decreasing the elution time by a factor of 2). This is important as the total time for one elution is very long for FPLC columns, ranging from 10 to 40 hours, and only one column can be run at a time. We therefore use 60 psi as the pressure for other tests with the FPLC unit.

Acid molarity. We tested the effect of acid molarity for both AG50W-X8 resin (Fig. 5C and D; 120 cm FPLC columns) and AG50W-X12 resin (Fig. 6C and D; 150 cm FPLC columns). For AG50W-X8 resin, two acid molarities of 0.5 and 1 M HNO_3 were used. Compared to the elution using 0.5 M HNO_3, the elution using 1 M HNO_3 required only half the volume of the 0.5 M HNO_3 to elute the alkali metals. For example, Rb was eluted from the column when ~60 mL 0.5 M HNO_3 was passed through the column, while the volume was ~30 mL when 1 M HNO_3 was used. This is consistent with the distribution coefficients reported by Strelow *et al.*[39] showing that higher acid molarity is associated with lower distribution coefficients. Similar to AG50W-X8 resin, AG50W-X12 resin also shows a decrease in distribution coefficients at higher acid molarity. In terms of alkali metal separation, the 0.5 and 1 M HNO_3 elutions were broadly similar for the AG50W-X8 resin ($R = 0.88$ for both, and the flow rates are also similar, ~4 cm min^{-1}; Fig. 5C and D). However, the tests with AG50W-X12 resin showed that a lower acid molarity (0.7 M HNO_3) led to a much better separation of Rb from K ($R = 1.91$; Fig. 6C) than the higher acid molarity (1 M HNO_3; $R = 1.05$; Fig. 6D), at similar flow rates of 2.9 and 3.2 cm min^{-1} (60 psi or 4.1 bar pressure drop), respectively.

Resin cross-linkage. Previous work on cation resins of X2, X8, and X16 cross-linking suggests that in general the selectivity (resolution) of alkali metals increases with the increase in resin cross-linkage.[46] Here we compare the AG50W-X8 and the AG50W-X12 resin. In general, the AG50W-X12 resin (Fig. 6) resulted in a better separation compared to AG50W-X8 resin (Fig. 5). In the tests done with the AG50W-X8 resin, Rb and K were never completely separated from each other ($R < 1$), and the best separation was achieved using a 120 cm-long column run at 60 psi (4.1 bar) and room temperature ($R = 0.88$; flow rate = 4 cm min^{-1}; acid molarity = 0.5–1 M; Fig. 5C and D). For the AG50W-X12 resin, a 130 cm column run under the same pressure drop yielded a complete separation of Rb from K ($R = 1.64$; flow rate = 3 cm min^{-1}; acid molarity = 0.8 M; Fig. 6A). The column lengths are

slightly different in the two tests (120 cm for AG50W-X8 resin *vs.* 130 cm for AG50W-X12 resin), this is because the two columns were made at different times, and the different cross-linkages of the two resins made it difficult to match the exact same length due to their different shrinkage. However, this difference in length is fairly small compared to the total length of the columns (*i.e.*, less than 10% difference), and the effect should be negligible. The acid molarity was also slightly different for the 120 cm (1 M HNO_3; Fig. 5C and D) and 130 cm (0.8 M HNO_3; Fig. 6A) columns. As discussed above, the 0.5 M HNO_3 and 1 M HNO_3 yielded similar results for AG50W-X8 resin ($R = 0.88$; Fig. 5C and D). It is thus expected that with an intermediate 0.8 M HNO_3, the separation should be similar (*i.e.*, R should be around 0.88). In comparison, the AG50W-X12 column in 0.8 M resulted in a complete separation between Rb and K ($R = 1.64$; Fig. 6A). This suggests that the higher resin cross-linkage helped the separation.

Temperature. The effect of temperature was tested using a 130 cm FPLC column filled with AG50W-X12 resin (Fig. 6A and B). Two elutions at room temperature (~20 °C) and 70 °C were performed under a pressure drop of 60 psi (4.1 bar). Temperature can affect several aspects of an elution: (i) it can affect resin/fluid distribution coefficients, (ii) higher temperature promotes faster equilibration between the resin and the eluent, thus lowering the HETP and resulting in a better separation, and (iii) higher temperature can accelerate vertical diffusion and thus increase the HETP.[46] Our tests showed that the separation of Rb from K at 70 °C ($R = 0.65$) was much worse than that at 20 °C ($R = 1.64$). A possible explanation for such a negative effect of temperature is a faster longitudinal diffusion of elements at higher temperature, resulting in an increase in the HETP. Calculation of the HETP indeed suggests an increase in the plate height (0.14 cm for 20 °C *vs.* 0.26 cm for 70 °C; Table 2). However, the flow rates at the two temperatures are quite different, about 3 cm min^{-1} at 20 °C and 5.7 cm min^{-1} at 70 °C, despite of the same pressure drop of 60 psi (4.1 bar). Therefore, an alternative explanation would be that the difference is mainly caused by the contrast in flow rates. At the current stage, we cannot tell which explanation is correct. We can, however, conclude that increasing temperature does not help with the separation at a fixed pressure, and ambient temperature should be used.

In summary, our tests show that, (i) longer columns and lower acid molarity result in a better separation, (ii) the higher cross-linkage cation resin AG50W-X12 yields better separations than AG50W-X8, and (iii) faster flow rates associated with higher pressure drop and/or temperature have negative impacts on the separation. Among all the tests on cation-exchange resins AG50W-X8 (Fig. 4 and 5) and AG50W-X12 (Fig. 6), the columns that successfully separated Rb from K were the 130 and 150 cm AG50W-X12 resin columns run at room temperature and a pressure drop of 60 psi (4.1 bar; linear flow rate of ~3 cm min^{-1}) (Fig. 6A, C, and D), and the best result was achieved with the 150 cm AG50W-X12 resin column using 0.7 M HNO_3 for elution (Fig. 6C).

3.3 Rubidium and potassium purification using Sr resin

The distribution coefficients of alkali metal elements on Sr resin[42] suggest that the largest separation between Rb and K occurs at ~2–3 M HNO_3. An advantage of using Sr-spec resin for Rb separation is that in 2–3 M HNO_3, the Sr distribution coefficient is higher than 100,[42] meaning that it is strongly partitioned onto the resin. Therefore, a low Sr/Rb can be easily achieved in the recovered Rb aliquot. As discussed in Sect. 2.5, a low Sr/Rb ratio is crucial for Rb isotopic analysis because ^{87}Sr is an isobar of ^{87}Rb, and a correction of ^{87}Rb by monitoring ^{88}Sr is only effective for a $^{88}Sr/^{85}Rb$ intensity ratio (volt/volt) lower than 0.001.[14]

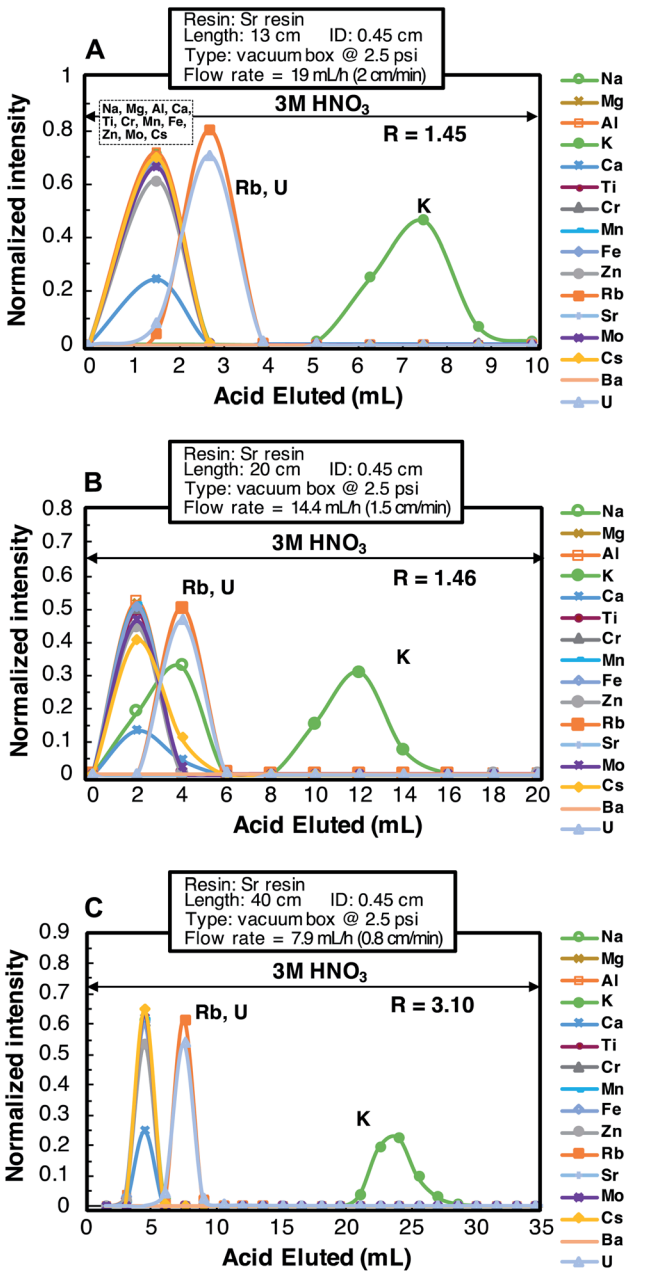

Fig. 7 Elution curves of Sr resin as a function of column length. Resolution R was calculated based on the separation between Rb and K peaks. All the tests were set at a pressure drop of 2.5 psi (~0.17 bar). The flow rate decreases with increasing length, while the resolution increases. Panel C is modified from ref. 14.

Using Sr resin to purify Rb was done in two previous studies,[14,28] which used 3 M HNO_3 as the eluent, but with different column lengths. Therefore, we compare how column lengths influence K and Rb separation. About 100 μL of a ~100 μg g^{-1} multi-element solution was loaded onto the Sr resin columns of three different lengths (13, 20, and 40 cm, with an ID of 0.45 cm) for measuring elution curves. A vacuum box was used to accelerate the flow rate by setting the pressure drop to 2.5 psi (~0.2 bar). The three columns resulted in different flow rates of 2, 1.5, and 0.8 cm min^{-1}, and different resolutions between Rb and K peaks of 1.45, 1.46, and 3.1, respectively (Fig. 7).

Compared to cation-exchange resins, the Sr resin can separate Rb from K more efficiently, and no overlap between Rb and K peaks was observed for the three column lengths. However, the Rb peak overlaps largely with the peaks of other matrix elements on the 13 and 20 cm columns, while the 40 cm column yields better separation of Rb from these elements. Given the overlap between Rb and matrix elements, the Sr resin column could be used as the last clean-up step for Rb and K purification, provided that the matrix elements are removed previously by other columns.

4. Discussion

4.1 Comparison between AMP-PAN resin, cation-exchange resins, and Sr resin

Complete separation of Rb from K is achievable with all three resins (AMP-PAN resin, cation resins, and Sr resins), and the yields for Rb are >95% in all cases. However, all resins have advantages and disadvantages. For AMP-PAN resin, the procedural blank of Rb is very high (~80 ng) compared to the other two procedures using cation-exchange resins (~6 ng) and Sr resin (~0.1 ng). This blank level can be problematic if AMP-PAN resin is used to separate Rb from Rb-depleted samples. For example, dissolving ~100 mg lunar mare basalt yields ~100 ng Rb (assuming a Rb concentration of ~1 μg g^{-1}), and 80 ng Rb blank would account for ~45% of total Rb after purification. The high Rb blank is primarily from two sources: ammonium solution (NH_4Cl solution) used for Rb elution, and the AMP-PAN resin itself, which was heated to 70 °C to increase the yield of Rb to >95% by partially decomposing the resin. The high blank may be counterbalanced by using a large amount of material, then the resin capacity needs to be considered. We did not measure the resin capacity for Rb, but previous work have determined the resin capacity for Cs, which is 64 mg Cs per g dry resin.[47] Assuming that Rb and Cs occupy the same sites in the resin, and because they have the same valence, the resin capacity for Cs would translate to ~40 mg Rb per g dry resin. We use 1 mL columns (approximately 0.3 g dry resin), so the column capacity would be ~12 mg Rb. For column chromatography, the loading amount should be much less than the resin capacity to avoid breakthrough. Taking 10% total capacity, one can load about 1 mg Rb, which would translate to ~20 g terrestrial basalts (assuming a 50 μg g^{-1} Rb concentration, as in geostandard BCR-1). One would also need to take into account matrix elements occupying resin sites when loading a sample, but overall the resin only has a high selectivity for Rb and Cs and not for matrix elements (Fig. 2 and 3). Therefore, resin capacity does not seem to be a limiting factor for using the resin. Rather, the high blank requires the loaded Rb amount to be high enough so that the blank does not contribute much to the total Rb. To make the contribution of blank less than 10%, the loaded Rb should be higher than 720 ng (*i.e.*, 80/(80 + 720) = 10%).

Rubidium cannot be effectively separated from K using only cation-exchange resins in gravity-driven columns. Overlaps between Rb and K peaks were observed for all gravity-driven columns tested in this study, which have column lengths varying from 6.8 to 20 cm and were filled with AG50W-X8 resin (200–400 mesh). Theoretically, longer columns would result in a better separation, but increasing the column length would decrease the flow rate and lead to a more tedious elution (the elution time of the 20 cm gravity-driven column was ~30 h). This can be mitigated by increasing the flow rate through a higher pressure drop (using a vacuum box or FPLC) or a higher temperature (using FPLC). Higher flow rates, however, have a negative impact on the separation. Thus, there is a trade-off between column length and flow rate (pressure drop). Complete separation of Rb from K was achieved with 130 and 150 cm columns filled with AG50W-X12 resin, run at a pressure drop of 60 psi (4.1 bar) at room temperature, with a flow rate of 3 cm min^{-1} (Fig. 6). We took advantage of the FPLC system available in the lab, which can pressurize the top of a column to run long columns, but the FPLC system is not commercially available, and therefore the FPLC procedure cannot be easily conducted in other laboratories. Another disadvantage with the long columns is that the elution time is very long, ~40 hours for one complete elution and another 20 hours for cleaning the column. Additionally, only one column can be run through the FPLC unit each time.

The Sr resin provides the most straightforward way for separating Rb from K among the three resins investigated. The Rb and K peaks were fully separated from each other even with short Sr resin columns (~13 cm in length). The only disadvantage is that the resin is rather expensive and cannot be recycled many times (2- or 3-times re-use is however feasible[28]).

4.2 Complete procedures for Rb and K purification on natural samples

Each of the three resins can purify Rb from K, the most difficult part of Rb separation, but they do not necessarily separate Rb and K from other matrix elements at the same time. In order to separate Rb and K simultaneously, additional columns are required to remove the matrix elements first. We have developed three complete chemical procedures using the three different resins to extract Rb (and K) from rock samples for isotopic analysis by MC-ICPMS. The main motivation for doing so was to assess the accuracy of Rb isotopic analyses of selected geostandards, which can be used in future studies for ground-truthing Rb isotopic analyses of samples with unknown compositions. The three procedures are outlined in Table 1: (i) the AMP-PAN resin method includes a first column using AMP-

PAN resin to separate Rb from K and other matrix elements, followed by a second anion-exchange resin AG1-X8 column to remove Mo in the Rb eluent that comes from the AMP-PAN resin, (ii) the cation-exchange resins + FPLC method uses three columns. The first is a gravity-driven AG50W-X8 column that is used to separate Rb and K from matrix elements, the second is an anion-exchange resin column to remove Ti whose elution peak overlaps with K and Rb peaks in the previous step, and the third is a FPLC long column of 150 cm length filled with AG50W-X12 resin to separate Rb and K from each other, and (iii) the Sr resin method follows Nie and Dauphas,[14] which uses first a column filled with cation-exchange resin AG50W-X8 to separate Rb and K from matrix elements, followed by a column of anion-exchange resin AG1-X8 to further purify Rb and K by removing matrix element Ti, then followed by a Sr resin column to separate Rb and K from each other. All three methods completely separate Rb from K, and for methods (ii) and (iii), K was purified at the same time (both methods quantitatively recover K with a low K blank of less than 20 ng), and can be used for K isotopic analysis.

4.3 Applications to synthetic and natural samples

We tested the reliability of the three Rb purification methods in the determination of Rb isotopic compositions by MC-ICPMS using natural and synthetic samples. The samples (Table 3) include the Rb isotopic reference standard SRM984 and several geostandards. The geostandards comprised three basalts (BCR-2, BHVO-2, BE-N), one andesite (AGV-2), and three granites (GS-N, G-3, G-A). Additionally, we doped two Rb-depleted (Rb concentration of ~0.5 μg g^{-1}) peridotite/dunite geostandards (PCC-1/DTS-2b) with the SRM984 solution to produce a mixture in which less than 1% of the total Rb derives from the rocks. The rationale for this was to process samples with a known Rb isotopic composition but with chemical compositions of natural rocks.

We digested these samples in various mixtures of HF–HNO_3–HCl–$HClO_4$ acids, following the protocol used by Nie and Dauphas.[14] Briefly, the samples were first dissolved in a mixture of concentrated HF–HNO_3 (2 : 1 in volume) with a few drops of $HClO_4$ on a hotplate at 130 °C. The sample solutions were then dried at ~170 °C (for evaporating $HClO_4$), re-dissolved in aqua regia (3 : 1 volume mixture of concentrated HCl–HNO_3) at 130 °C for another 24 h. After repeating the aqua regia step for a second time, the samples were re-dissolved in sample loading media for columns. We separated Rb from these samples using the three methods above (Table 1) and measured the Rb isotopic compositions using MC-ICPMS. The obtained Rb isotopic compositions of the samples are reported in Table 3. The δ^{87}Rb values of the geostandards agree well with the values reported previously.[12,14,28] For the samples that were purified using more than one Rb separation method from this study, the δ^{87}Rb values are compared in Fig. 8. We applied the AMP-PAN method to only Rb-enriched samples of synthetic ones and granites because of its high Rb blank (~80 ng), but the tests of

Table 3 Rubidium isotopic compositions of geostandards and synthetic samples using the three different purification procedures in Table 1

Samples	Rock type	δ^{87}Rb (‰)$_{SRM984}$	95% c.i.	n^b
(1) AMP-PAN resin method (Rb blank of ~80 ng, Rb yield >95%)				
SRM984	Reference standard	−0.02	0.03	10
SRM984 + PCC-1(I)[a]	Mixture of reference standard and Rb-depleted peridotite	−0.02	0.03	10
SRM984 + PCC-1(II)[a]	Mixture of reference standard and Rb-depleted peridotite	−0.05	0.03	10
GS-N	Granite	−0.20	0.03	10
G-3	Granite	−0.28	0.03	10
(2) Cation-exchange resins + FPLC (Rb blank of ~6 ng, Rb yield >95%)				
SRM984	Reference standard	0.03	0.03	9
SRM984 + DTS-2b	Mixture of reference standard and Rb-depleted dunite	−0.02	0.03	7
BCR-2 (I)[a]	Basalt	−0.16	0.01	9
BCR-2 (II)[a]	Basalt	−0.15	0.01	9
BHVO-2	Basalt	−0.11	0.01	9
BE-N	Basalt	−0.10	0.02	9
AGV-2	Andesite	−0.13	0.02	9
GS-N	Granite	−0.14	0.05	8
G-3	Granite	−0.24	0.01	9
G-A	Granite	−0.22	0.03	9
(3) Sr resin method (Rb blank of ~0.1 ng, Rb yield >95%)				
SRM984 + PCC-1	Mixture of reference standard and Rb-depleted peridotite	−0.02	0.04	9
BCR-2	Basalt	−0.16	0.02	9
BHVO-2	Basalt	−0.12	0.02	9
AGV-2	Andesite	−0.15	0.02	9
GS-N	Granite	−0.19	0.02	9
G-3	Granite	−0.23	0.03	7

[a] (I) and (II) denote different digestions. $\delta^{87}Rb$ is defined as: $\delta^{87}Rb = [(^{87}Rb/^{85}Rb)_{sample}/(^{87}Rb/^{85}Rb)_{SRM984} - 1] \times 1000$. [b] n is the number of replicate analyses.

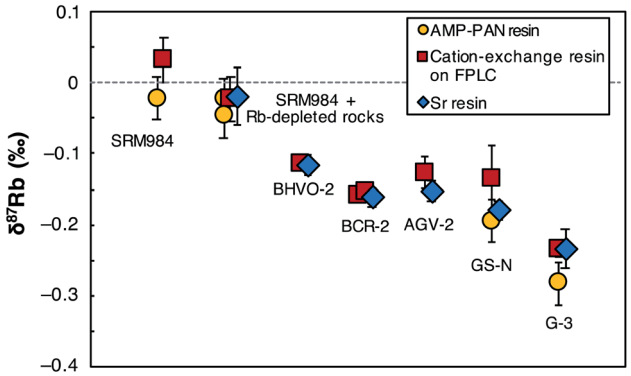

Fig. 8 Rubidium isotopic compositions of synthetic samples and geostandards, obtained using AMP-PAN method, cation-exchange resins + FPLC method, and Sr resin method (Table 1). The three methods yield consistent results. The AMP-PAN method was only applied to Rb-enriched samples such as the synthetic ones and granites due to its high Rb blank of ~80 ng. The cation-exchange resin + FPLC method and the Sr resin method have lower blanks of ~6 ng and ~0.1 ng, respectively, and can be applied to low-Rb samples. The latter two also simultaneously separate K that can be used for K isotopic analysis using MC-ICPMS.

the cation-exchange resins + FPLC method and the Sr resin method (with Rb blank levels of ~6 and ~0.1 ng, respectively) were extended to also relatively low-Rb andesites and basalts. The three methods produced δ^{87}Rb values that agree within uncertainties (Fig. 8).

The high-blank problem of AMP-PAN resin could be alleviated by increasing the sample mass processed with chromatography chemistry. Terrestrial crust is enriched in Rb because alkali elements are incompatible during magmatic differentiation, but samples from other planetary bodies (*e.g.*, lunar samples and chondrites) have Rb concentrations by a factor of ~100 lower. Therefore, despite the fact that the AMP-PAN resin can separate Rb from K efficiently with only a small 1 mL resin column, the method might only be suitable for high-Rb terrestrial samples. In contrast, the cation-exchange resins + FPLC method and the Sr resin method do not have blank issues and can be applied to Rb-depleted samples. The latter two methods also separate K simultaneously, whose isotopic composition can be measured by MC-ICPMS. As discussed above, however, the cation-exchange resins + FPLC method would require a FPLC system that is not commercially available. Therefore, the Sr resin method is the most efficient and easily implementable method to separate both Rb and K for isotopic analysis of these two elements.

5. Conclusion

We tested the effectiveness of three types of resins that have been used to purify Rb from K and matrix elements prior to isotopic analysis by MC-ICPMS, including AMP-PAN resin, cation-exchange resins, and Sr resin. We find that the AMP-PAN resin is highly effective in separating Rb from K and other matrix elements, but it has a high Rb blank (~80 ng) and is tedious to implement.

We tested the effect of column length, acid molarity, temperature, pressure drop (flow rate), and resin cross-linkage on Rb and K separation using cation-exchange resins. Increasing column length helps the separation, while increasing acid molarity, temperature, or pressure drop (flow rates) has negative impacts on the separation. Complete separation of Rb from K was not achieved using gravity-driven AG50W-X8 columns with column lengths ranging from 6.8 cm to 20 cm. Increasing column length and resin cross-linkage from AG50W-X8 to AG50W-X12 has positive effects on the separation. Complete separation of Rb from K was achieved using AG50W-X12 resin filled in a column of 0.16 cm inner diameter and 150 cm length installed in a FPLC system, run at room temperature and a flow rate of 3 cm min^{-1} (60 psi or 4.1 bar pressure drop). The Rb blank of the procedure using cation resins to purify Rb is ~6 ng.

The Sr resin can cleanly and efficiently separate Rb from K, and a relatively short column (13–40 cm in length) is sufficient. The Rb blank of the separation procedure using this resin is only ~0.1 ng. Therefore, Sr resin is the optimal choice among the three resins to separate Rb from K.

Three chemical procedures for the separation of Rb from natural samples using the three resins were designed (Table 1), and tested with synthetic solutions and natural rocks. We measured the Rb isotopic compositions of purified Rb solutions from those tests using MC-ICPMS. The three procedures yielded consistent Rb isotopic compositions. The cation-exchange resins + FPLC procedure and the Sr resin procedure allow purification of both Rb and K from single digestion aliquots, and can be applied to a large variety of terrestrial and meteorite samples for combined Rb and K isotopic studies.

Conflicts of interest

There are no conflicts to declare.

Acknowledgements

This work was supported by a NASA NESSF fellowship (NNX15AQ97H), a Carnegie postdoctoral fellowship, and a Carnegie Postdoc × Postdoc (P^2) seed grant to NXN, NASA grants NNX17AE86G, NNX17AE87G, 80NSSC17K0744, 80NSSC20K0821, and NSF grant EAR-2001098 to ND.

References

1 E. L. Garner, L. A. Machlan and I. L. Barnes, *Lunar and Planetary Science Conference Proceedings*, 1975, vol. 6, pp. 1845–1855.
2 M. Humayun and R. N. Clayton, *Geochim. Cosmochim. Acta*, 1995, **59**, 2115–2130.
3 C. M. O. Alexander, J. N. Grossman, J. Wang, B. Zanda, M. Bourot-Denise and R. H. Hewins, *Meteorit. Planet. Sci.*, 2000, **35**, 859–868.
4 J. S. Pistiner and G. M. Henderson, *Earth Planet. Sci. Lett.*, 2003, **214**, 327–339.

5 C. M. O. Alexander and J. N. Grossman, *Meteorit. Planet. Sci.*, 2005, **40**, 541–556.
6 O. Nebel, K. Mezger and W. van Westrenen, *Earth Planet. Sci. Lett.*, 2011, **305**, 309–316.
7 S. Misra and P. N. Froelich, *Science*, 2012, **335**, 818–823.
8 P. A. P. Von Strandmann, H. C. Jenkyns and R. G. Woodfine, *Nat. Geosci.*, 2013, **6**, 668–672.
9 P. B. Tomascak, T. Magna and R. Dohmen, *Advances in Lithium Isotope Geochemistry*, Springer, 2016.
10 K. Wang and S. B. Jacobsen, *Nature*, 2016, **538**, 487–490.
11 S. Penniston-Dorland, X.-M. Liu and R. L. Rudnick, *Rev. Mineral. Geochem.*, 2017, **82**, 165–217.
12 E. A. Pringle and F. Moynier, *Earth Planet. Sci. Lett.*, 2017, **473**, 62–70.
13 S. Li, W. Li, B. L. Beard, M. E. Raymo, X. Wang, Y. Chen and J. Chen, *Proc. Natl. Acad. Sci. U. S. A.*, 2019, **116**, 8740–8745.
14 N. X. Nie and N. Dauphas, *Asia Pac. J. Life Sci.*, 2019, **884**, L48.
15 H. D. Hanna, X.-M. Liu, Y.-R. Park, S. M. Kay and R. L. Rudnick, *Geochim. Cosmochim. Acta*, 2020, **278**, 322–339.
16 Y. Hu, F.-Z. Teng, T. Plank and C. Chauvel, *Sci. Adv.*, 2020, **6**, eabb2472.
17 P. Koefoed, O. Pravdivtseva, H. Chen, C. Gerritzen, M. M. Thiemens and K. Wang, *Meteorit. Planet. Sci.*, 2020, **55**, 1833–1847.
18 H. Bloom, K. Lodders, H. Chen, C. Zhao, Z. Tian, P. Koefoed, M. K. Pető, Y. Jiang and K. Wang, *Geochim. Cosmochim. Acta*, 2020, **277**, 111–131.
19 Y. Jiang, P. Koefoed, O. Pravdivtseva, H. Chen, C.-H. Li, F. Huang, L.-P. Qin, J. Liu and K. Wang, *Meteorit. Planet. Sci.*, 2021, **56**, 61–76.
20 Y. Hu, F.-Z. Teng and C. Chauvel, *Geochim. Cosmochim. Acta*, 2021, **295**, 98–111.
21 Z. J. Zhang, N. X. Nie, R. A. Mendybaev, M.-C. Liu, J. J. Hu, T. Hopp, E. E. Alp, B. Lavina, E. S. Bullock and K. D. McKeegan, *ACS Earth Space Chem.*, 2021, **5**(4), 755–784.
22 K. Wang and S. B. Jacobsen, *Geochim. Cosmochim. Acta*, 2016, **178**, 223–232.
23 W. Li, X.-M. Liu and L. V. Godfrey, *Geostand. Geoanal. Res.*, 2019, **43**, 261–276.
24 G. Zhu, J. Ma, G. Wei and L. Zhang, *Front. Chem.*, 2020, **8**, 557489.
25 K. S. Heier and J. A. Adams, *Phys. Chem. Earth*, 1964, **5**, 253–381.
26 Y. Hu, X.-Y. Chen, Y.-K. Xu and F.-Z. Teng, *Chem. Geol.*, 2018, **493**, 100–108.
27 J. F. Rudge, B. C. Reynolds and B. Bourdon, *Chem. Geol.*, 2009, **265**, 420–431.
28 Z. Zhang, J. Ma, L. Zhang, Y. Liu and G. Wei, *J. Anal. At. Spectrom.*, 2018, **33**, 322–328.
29 T. Waight, J. Baker and B. Willigers, *Chem. Geol.*, 2002, **186**, 99–116.
30 O. Nebel, K. Mezger, E. Scherer and C. Münker, *Int. J. Mass Spectrom.*, 2005, **246**, 10–18.
31 H. Zeng, V. F. Rozsa, N. X. Nie, Z. Zhang, T. A. Pham, G. Galli and N. Dauphas, *ACS Earth Space Chem.*, 2019, **3**, 2601–2612.
32 J. v. R. Smit, W. Robb and J. J. Jacobs, *J. Inorg. Nucl. Chem.*, 1959, **12**, 104–112.
33 C. J. Coetzee, *J. Chem. Educ.*, 1972, **49**, 33.
34 J. v. R. Smit, J. J. Jacobs and W. Robb, *J. Inorg. Nucl. Chem.*, 1959, **12**, 95–103.
35 K. Brewer, T. Todd, D. Wood, P. Tullock, F. Sebesta, J. John and A. Motl, *Czech. J. Phys.*, 1999, **49**, 959–964.
36 T. J. Ireland, F. L. H. Tissot, R. Yokochi and N. Dauphas, *Chem. Geol.*, 2013, **357**, 203–214.
37 H. Li, F. L. Tissot, S.-G. Lee, E. Hyung and N. Dauphas, *ACS Earth Space Chem.*, 2020, **5**, 55–65.
38 F. W. E. Strelow, *Anal. Chem.*, 1960, **32**, 1185–1188.
39 F. W. Strelow, R. Rethemeyer and C. J. C. Bothma, *Anal. Chem.*, 1965, **37**, 106–111.
40 N. Dauphas, F. L. H. Tissot, R. Yokochi and T. J. Ireland, Pneumatically/hydraulically actuated fluoropolymer-hplc chromatographic system for use with harsh reagents, *US Pat.*, US20150008171A1, 2015.
41 J. Y. Hu, N. Dauphas, F. L. H. Tissot, R. Yokochi, T. J. Ireland, Z. Zhang, A. M. Davis, F. J. Ciesla, L. Grossman, B. L. A. Charlier, M. Roskosz, E. E. Alp, M. Y. Hu and J. Zhao, *Sci. Adv.*, 2021, **7**, eabc2962.
42 E. Philip Horwitz, R. Chiarizia and M. L. Dietz, *Solvent Extr. Ion Exch.*, 1992, **10**, 313–336.
43 A. J. Martin and R. L. Synge, *Biochem. J.*, 1941, **35**, 1358–1368.
44 J. J. van Deemter, F. J. Zuiderweg and A. Klinkenberg, *Chem. Eng. Sci.*, 1956, **5**, 271–289.
45 L. R. Snyder, J. J. Kirkland and J. W. Dolan, *Introduction to Modern Liquid Chromatography*, John Wiley & Sons, 2011.
46 R. Dybczyński, *J. Chromatogr. A*, 1972, **72**, 507–522.
47 R. S. Herbst, J. D. Law, T. A. Todd, D. Wood, T. G. Garn and E. L. Wade, *Integrated AMP-PAN, TRUEX, and SREX Flowsheet Test to Remove Cesium, Surrogate Actinide Elements, and Strontium from INEEL Tank Waste Using Sorbent Columns and Centrifugal Contactors*, Idaho National Laboratory (INL), 2000.
48 Z Zhang, J Ma, Z Wang, L Zhang, X He, G Zhu, T Zeng and G Wei, *Geochim. Cosmochim. Acta*, 2021, **313**, 99–115.

